Catalytic Effect of Nanoparticle 3d-Transition Metals on Hydrogen Storage Properties in Magnesium Hydride MgH_2 Prepared by Mechanical Milling

Nobuko Hanada,*,† Takayuki Ichikawa,‡ and Hironobu Fujii‡

Graduate School of Advanced Sciences of Matter, Hiroshima University, 1−3−1 Kagamiyama, Higashi-Hiroshima 739-8530, Japan, and Natural Science Center for Basic Research and Development, Hiroshima University, 1-3-1 Kagamiyama, Higashi-Hiroshima 739-8526, Japan

Received: November 29, 2004; In Final Form: February 15, 2005

We examined the catalytic effect of nanoparticle 3d-transition metals on hydrogen desorption (HD) properties of MgH_2 prepared by mechanical ball milling method. All the MgH_2 composites prepared by adding a small amount of nanoparticle Fe^{nano}, Co^{nano}, Ni^{nano}, and Cu^{nano} metals and by ball milling for 2 h showed much better HD properties than the pure ball-milled MgH_2 itself. In particular, the 2 mol % Ni^{nano}-doped MgH_2 composite prepared by soft milling for a short milling time of 15 min under a slow milling revolution speed of 200 rpm shows the most superior hydrogen storage properties: A large amount of hydrogen (∼6.5 wt %) is desorbed in the temperature range from 150 to 250 °C at a heating rate of 5 °C/min under He gas flow with no partial pressure of hydrogen. The EDX micrographs corresponding to Mg and Ni elemental profiles indicated that nanoparticle Ni metals as catalyst homogeneously dispersed on the surface of MgH_2. In addition, it was confirmed that the product revealed good reversible hydriding/dehydriding cycles even at 150 °C. The hydrogen desorption kinetics of catalyzed and noncatalyzed MgH_2 could be understood by a modified first-order reaction model, in which the surface condition was taken into account.

1. Introduction

Magnesium hydride MgH_2 is one of the attractive hydrogen storage materials because it is directly formed from the reaction of Mg metal with gaseous hydrogen and reaches a high hydrogen capacity (∼7.6 wt %). However, the reaction is too slow for practical use and needs higher temperature than 300 °C for progressing hydrogen absorption and desorption reactions.[1−3]

Recently, the hydrogen storage (H-storage) properties of the composites composed of Mg or MgH_2 and a small amount of transition metals Ti, V, Mn, Fe, Co, Ni, Cu and Pd or transition metal oxides has been studied to improve the hydriding/dehydriding kinetics without reducing its high hydrogen capacity.[4−18]

Liang et al. have reported some good H-storage properties of MgH_2 with 5 mol % transition microparticle metals (Ti, V, Mn, Fe, and Ni) milled for 20 h,[4−8] in which the composite with V desorbed ∼5 wt % hydrogen within 200 s at 300 °C under a hydrogen pressure of 0.015 MPa. Furthermore, Zaluska et al. have studied H-storage properties of Mg composites prepared by ball milling with 1 wt % transition microparticle metals (corresponding to 0.3 mol % Pd and 0.5 mol % Fe doping), and ∼6 wt % of hydrogen was desorbed at 330 °C within 30 min (1800 s) under a hydrogen pressure of 0.1 MPa.[9] They claimed that the doped metals uniformly distributed on the magnesium surface in the form of nanoparticles. This indicates that when very small size particles (diameter of several tens of nanometers) of the metal catalyst are uniformly distributed on the Mg surface, even a small amount of catalyst is sufficient for improving the reaction kinetics. Recently, Kanoya et al. have investigated H-storage properties of some ball milled Mg with a small amount of nanometer sized metals (Ni and Fe) as catalyst.[10] Their results indicated that a Mg−0.33Ni−0.17Fe (at. %) composite prepared by ball milling for only 15 min could absorb and desorb 7.49 wt % of hydrogen at 350 °C.

On the other hand, Oelerich et al. have reported some catalytic effects of the transition microparticle metal oxides for MgH_2.[11−14] The MgH_2 composites prepared by ball milling for 100 h with 0.2 mol % Nb_2O_5 revealed the best H-storage properties among all the metal oxide catalysts: ∼7 wt % of hydrogen was desorbed within 150 s at 300 °C under vacuum.[14]

In our group, it has been clarified that Pd-coated nanostructured Mg films prepared by a RF sputtering method absorbed ∼5 wt % of hydrogen at 373 K under hydrogen atmosphere of 0.1 MPa and completely desorbed below 373 K in a vacuum.[15−16] This indicates that MgH_2 is suitable for practical uses as well by modification of bulk MgH_2 into suitable nanostructure and catalyzing with suitable metals on it. In addition, we examined the correlation between H-storage properties and structural characteristics on the mechanically milled MgH_2 itself as a function of milling time, before studying the catalytic effect on H-storage properties of MgH_2.[19] The results indicated that at the early stage within 2 h milling, the amount of desorbed hydrogen decreased ∼16% from 7.3 to 6.1 wt % and the onset temperature of dehydrogenation decreased by 70 °C from 400 to 330 °C, while both the powder size and the crystallite size in powder decreased with increasing the milling time down to 1 μm and ∼10 nm, respectively. On the other hand, the lattice strain of 0.3% was quickly introduced, but it was completely released after 2 h milling. Finally, after 80 h of milling the hydrogen capacity and desorption temperature reached saturation for 6.5 wt % and 330 °C, while the crystalline size and the lattice strain reached saturation for ∼7 nm and again 0.2%, respectively.

* Corresponding author: E-mail: hanadan@hiroshima-u.ac.jp.
† Graduate School of Advanced Sciences of Matter.
‡ Natural Science center for Basic Research and Development.

10.1021/jp044576c CCC: $30.25
Published on Web 03/17/2005

At the next step of systematic studies of improving H-storage properties in Mg systems, in this paper, we examined the catalytic effect of nanometer-sized 3d-transition metals (Fe^{nano}, Co^{nano}, Ni^{nano}, and Cu^{nano}) on H-storage properties in MgH_2 prepared by mechanically milling method without exposing in air the products in all the preparing and measuring processes. The reason we used nanoparticle size metals as catalyst for MgH_2 is that they can be uniformly dispersed on the surface of MgH_2 by short ball milling and can avoid severe internal strains. As a result of such careful treatments, the obtained results indicated the most superior kinetic properties for hydrogen storage in the MgH_2 composites doped by 3d transition metals so far reported as far as we know.

2. Experimental Procedures

Magnesium hydride powder MgH_2 (the purity is 90 wt %, with several micrometer sizes, 9 wt % is unreacted Mg, and the remaining 1 wt % is due to impurities) was purchased from Sigma-Aldrich. The catalyst nanometer-particle metals Fe^{nano}, Co^{nano}, Ni^{nano}, and Cu^{nano} with diameters of several tens of nanometers and microparticle Ni^{micro} with a diameter of 3 μm were purchased from Shinku-Yakin Co. and Rare Metallic, respectively. The sizes of nanometer particles were determined by a TEM sampling method. In those nanometer-particle metals, any existence of the Ni, Fe, and Cu oxide phases went undetected by XRD examination. Only Co nanoparticles indicated the Co_3O_4 phase in addition to the pure Co metal phase. Prior to milling, a mixture of 300 mg of MgH_2 and 1−2 mol % Fe^{nano}, Co^{nano}, Ni^{nano}, and Cu^{nano} was put into a Cr steel pot (30 cm^3 in volume) together with 20 steel balls (7 mm in diameter). Then, after the pot was degassed below 1×10^{-4} Pa for 12 h, high-purity hydrogen gas (7 N) of 1.0 MPa was introduced into it. After then, the mixture was mechanically milled for 15 min∼2 h at 200−400 rpm using a planetary ball milling apparatus (Fritsch P7). The samples before and after milling were always handled in a glovebox filled with purified Ar gas so as to minimize the oxidation on the samples. It is to be noted that this treatment in a clean environment is also quite important to avoid surface oxidation.

The morphology of the composite particle was examined by scanning electron microscopy (SEM) observation (Hitachi S-2380N), and metal distribution on the milled particles was detected by the EDX equipment (EMAX-7000). The structural properties were examined by X-ray diffraction measurement (Rigaku RINT2500) using Cu Kα radiation. The hydrogen desorption (HD) properties of the products were examined by a thermal desorption mass spectroscope (TDMS) (Anelva M-QA200TS) in the heating process up to 450 °C with a heating rate of 5 °C/min under high-purity He gas (purity >99.9999%) flow with no partial pressure of hydrogen, in which a thermogravimeter (TG) (Rigaku TG8120) is also used. This equipment was specially designed and installed in a glovebox filled with purified Ar gas, so that the measurements of TDMS and TG could be achieved simultaneously without exposing the samples to air.

3. Results and Discussion

3.1. Catalytic Effect of Nanoparticle 3d-Transition Metals. Figure 1 shows profiles of thermal desorption mass spectra (TDMS) of hydrogen (H_2) for pure noncatalyzed MgH_2 and catalyzed MgH_2 composites with 1 mol % Fe^{nano}, Co^{nano}, Ni^{nano}, and Cu^{nano} nanoparticle metals prepared by ball milling for 2 h under a hydrogen gas pressure of 1 MPa. It can be seen that all the composites with nanoparticle metals as catalyst exhibit better hydrogen desorption properties than the pure MgH_2 by only 2 h milling: Their peak temperatures of hydrogen desorption are lower than that of pure MgH_2, and the amounts of desorbed hydrogen deduced from TG measurements are ∼7 wt % until 450 °C and almost the same as that of pure MgH_2 because only a small amount of nanoparticle metals (1 mol %) are added to MgH_2. Thus, we notice that a small amount of nanoparticle metals reveal a significant catalytic effect on the HD properties in MgH_2 without reducing its high hydrogen capacity. The Ni^{nano}-catalyzed MgH_2 composite shows the best hydrogen desorption properties among all the catalyzed MgH_2 composites and the peak temperature (260 °C) is about 100 °C lower than that of the pure milled MgH_2. In addition, it seems likely that these HD properties depend on the states of 3d-electorns because the peak temperature of hydrogen desorption decreases with increasing a number of occupied 3d-electrons on those transition metals except for Cu, which is known as one of the noncatalytic materials from the fact that the 3d-electron shell of Cu metal is fully occupied.[20] In the bottom of Figure 1, the TDMS profile of the MgH_2 composite milled with 1 mol % microparticle Ni^{micro} for 2 h is shown, for comparison with that of the 1 mol % Ni^{nano}- doped MgH_2 composite. It is noticed that the latter is much better than the former in the HD properties. This indicates that the smaller particle as a catalytic metal leads to better H-storage kinetic properties by short milling.

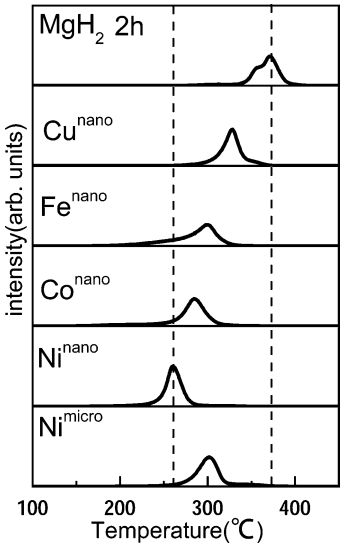

Figure 1. Thermal desorption mass spectra (TDMS) of hydrogen for pure MgH_2 milled for 2 h and catalyzed MgH_2 with 1 mol % Cu^{nano}, Fe^{nano}, Co^{nano}, and Ni^{nano} nanoparticle metals milled for 2 h at 400 rpm under He gas flow with no partial pressure of hydrogen. In this figure, TDMS profiles for MgH_2 with 1 mol % Ni^{micro} microparticle metals milled for 2 h at 400 rpm are also shown for comparison with that of the 1 mol % Ni^{nano}- catalyzed MgH_2 composite.

Figure 2 shows X-ray diffraction profiles for the MgH_2 composites with 1 mol % Fe^{nano}, Co^{nano}, Ni^{nano}, and Cu^{nano}. The main profiles for the above catalyzed samples exhibit the same peaks corresponding to β-MgH_2 and γ-MgH_2 as in the pure milled MgH_2. Except for the Co^{nano}-doped composite, small peaks corresponding to Ni, Fe, and Cu metals additionally exist in their patterns. Since Cu radiation is used in this work, the XRD method is not useful for the Co element in composites because the absorption cross section of Co element is the largest among the period 4 elements for Cu Kα radiation.

3.2. Optimization of Milling Conditions for the Ni Catalyst. As described above, the Ni^{nano}-catalyzed MgH_2 composite showed the best HD properties among the 3d-transition metal catalyzed composites. For optimizing the milling conditions, we next examined how the HD properties in the Ni^{nano}-catalyzed

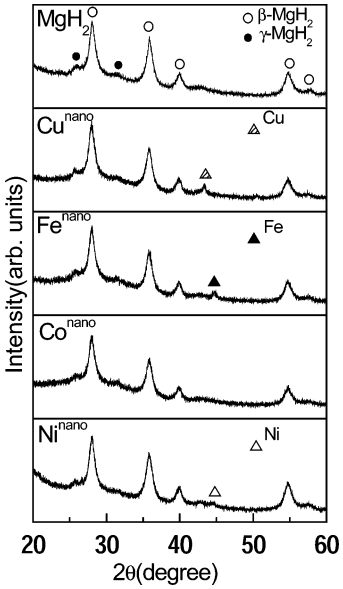

Figure 2. X-ray diffraction profiles for pure MgH_2 and catalyzed MgH_2 with 1 mol % Cu^{nano}, Fe^{nano}, Co^{nano}, and Ni^{nano} nanoparticle metals milled for 2 h at 400 rpm.

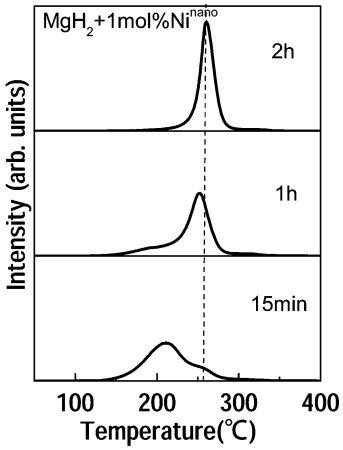

Figure 3. Thermal desorption mass spectra of hydrogen from the MgH_2 composites with 1 mol % Ni^{nano} in the milling conditions for 15 min, 1 h, and 2 h at 400 rpm.

system are kinetically improved by changing the milling time, the milling revolution speed, and the amount of Ni^{nano} catalyst.

First of all, the 1 mol % Ni^{nano}-catalyzed MgH_2 composite was prepared by changing the milling time from 15 min to 2 h at 400 rpm, and the TDMS profiles were examined. As shown in Figure 3, the milling for 1 h leads the onset temperature to about 150 °C, while the milling for 15 min leads the peak temperature to about 210 °C as well. Thus, the result indicates that the short time milling brings the better HD properties by using nanoparticle Ni^{nano} as catalyst. However, the TDMS profile shows a shoulder structure and widely distributes in the temperature range from 150 to 300 °C.

At the second step, the milling revolution speed from 400 to 200 rpm was changed under the condition of the short milling time for 15 min. In Figure 4, parts a and b, the TDMS profiles are shown for the 1 mol % Ni^{nano}-catalyzed MgH_2 composite milled at 400 and 200 rpm, respectively. It can be seen that the profile of the composite milled at 200 rpm reveals a single hydrogen desorption peak, but the desorption temperature range still widely distributes from 150 to 300 °C.

Finally, the amount of Ni^{nano} catalyst was increased from 1 to 2 mol % under the same conditions concerning with short

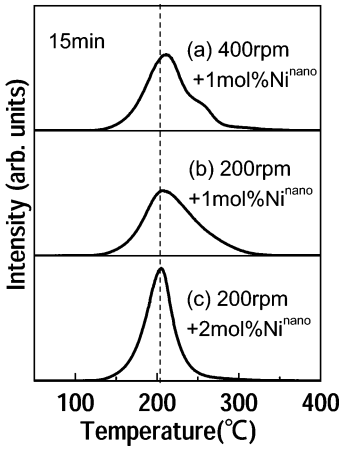

Figure 4. Thermal desorption mass spectra of hydrogen for the MgH_2 composites milled for 15 min at (a) 400 rpm with 1 mol % Ni^{nano}, (b) 200 rpm with 1 mol % Ni^{nano}, and (c) 200 rpm with 2 mol % Ni^{nano}, respectively.

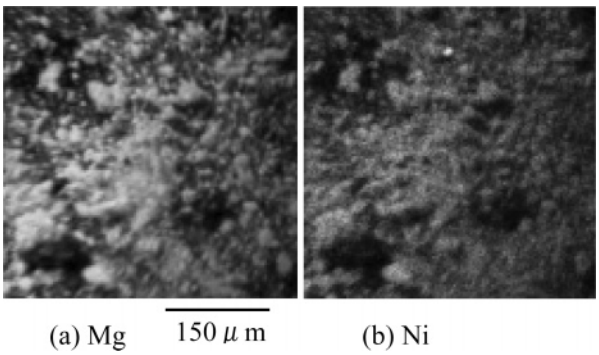

Figure 5. EDX micrographs of (a) Mg and (b) Ni elements in the MgH_2 composite with 2 mol % Ni^{nano} prepared by milling for 15 min at 200 rpm.

milling time for 15 min and the slow milling revolution speed at 200 rpm. As is shown in Figure 4 c, the MgH_2 composite with 2 mol % Ni^{nano} shows the most superior HD profile in the TDMS curves among all the composites examined in this work. Thus, it has been found that the 2 mol % Ni^{nano}-catalyzed MgH_2 prepared by the optimum condition desorbs a large amount of hydrogen (~6.5 wt %) in the temperature from 150 to 250 °C at the heating rate of 5 °C/min. From these results, it is concluded that the short milling time and slow milling revolution speed brings better HD properties for the 2 mol % Ni^{nano}-catalyzed MgH_2 composite.

To clarify the reason the HD kinetic properties for MgH_2 are so improved by a small amount of Ni^{nano} catalyst, the EDX micrographs corresponding to the Mg and Ni elemental profiles were examined for the optimum MgH_2 composite, i.e., 2 mol % Ni^{nano}-catalyzed MgH_2 milled for 15 min at 200 rpm, which is shown in Figure 5. It can be seen that the micrograph pattern of Mg is almost the same as that of Ni. This indicates that the Ni^{nano}-particles uniformly disperses on the surface of the several micrometer-sized MgH_2 particles by ball milling even for the short time and under the slow milling revolution speed.

3.3. Cyclic Properties of Hydrogenation/Dehydrogenation Reactions for the 2 mol % Ni^{nano}-Catalyzed MgH_2 Composite. Next, the cyclic properties of hydriding/dehydriding reactions were examined for the 2 mol % Ni^{nano}-catalyzed MgH_2 composite prepared by milling for 15 min at 200 rpm. The durability was tested by the following cyclic processes: the dehydrogenation was performed by keeping the composite under the following two different temperatures, (1) 150 °C (corresponding to the onset temperature for dehydrogenation) and (2)

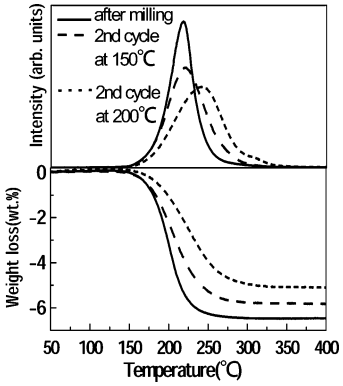

Figure 6. Thermal desorption mass spectra of hydrogen and TG profiles for the 2 mol % Ni^{nano} catalyzed MgH_2 composite prepared by milling for 15 min at 200 rpm. The solid line is the product after milling for 15 min at 200 rpm, the dashed line is for the sample after the second hydriding/dehydriding cycle at 150 °C and the dotted line for the sample after the second cycle at 200 °C.

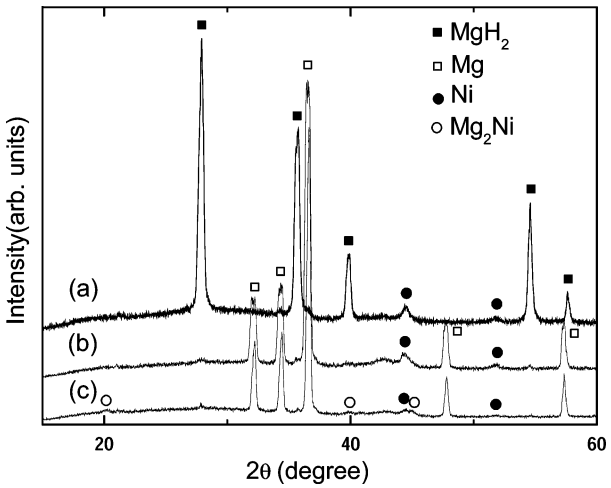

Figure 7. X-ray diffraction profiles for (a) the 2 mol % Ni^{nano}-catalyzed MgH_2 composite prepared after milling for 15 min at 200 rpm, (b) the product after dehydrogenation at 150 °C, and (c) the sample after dehydrogenation at 200 °C, respectively.

200 °C (corresponding to the peak temperature for dehydrogenation), for 12 h under high vacuum, respectively, while the hydrogenation was performed under pure hydrogen gas up to 3 MPa at (1) 150 and (2) 200 °C for 12 h, respectively, as well. After completing those (1 and 2) hydrogen absorbing/desorbing cycles, the HD properties were examined by TG-TDMS measurements. The results obtained are shown in Figure 6. The dehydrogenation property after second cycle at 150 °C is better than that after the second cycle at 200 °C in view of the temperature range of hydrogen desorption and the amount of desorbed hydrogen, but it is slightly worse than that after the first cycle. As is seen in Figure 7, parts a and b, the X-ray diffraction profiles indicate that both products after just milling and after dehydrogenating at 150 °C have a small peak corresponding to a pure Ni metal phase in addition to the main peaks for MgH_2 and Mg, respectively. On the other hand, as shown in Figure 7c for the product after dehydrogenation at 200 °C, there are the additional peaks corresponding to the Mg_2Ni phase. Since the catalytic effect of Mg_2Ni for improving the H-storage properties is weaker than Ni metal, the existence of Mg_2Ni in the Ni^{nano}-catalyzed MgH_2 composite would make the dehydrogenation properties worse.

This may be also the reason the short milling time and slow milling revolution speed brings better HD properties for Ni^{nano}-catalyzed MgH_2 in section 3.2. When the milling time and revolution speed are, respectively, too long and too high, the Mg_2Ni phase could be easily formed at the phase boundaries between Ni and main Mg phases because the affinity of Mg and Ni is very strong with each other. Thus, the formation of Mg_2Ni leads to worse HD properties with increasing milling time and milling revolution speed for MgH_2 as well.

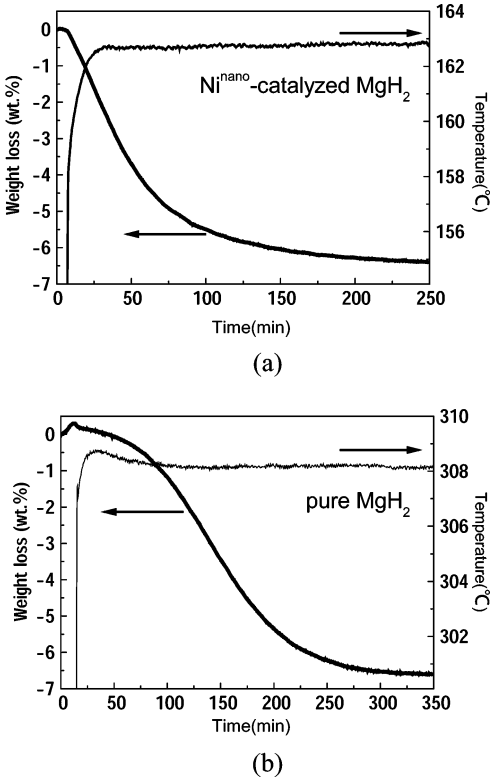

Figure 8. Weight loss due to hydrogen desorption and the aspect of temperature fluctuation around fixed temperatures as a function of HD reaction time for (a) the 2 mol % Ni^{nano}-catalyzed MgH_2 composite prepared by milling for 15 min at 200 rpm and (b) the pure MgH_2 milled for 15 min at 200 rpm, respectively.

3.4. Kinetics for Hydrogen Desorption (HD) Reaction in Pure MgH_2 and Ni^{nano}-Catalyzed MgH_2 Composite. In this work, the kinetics of the HD reaction was examined for the 2 mol % Ni^{nano}-catalyzed MgH_2 and pure noncatalyzed MgH_2 produced by ball milling for 15 min at 200 rpm. Figure 8 shows the amount of desorbed hydrogen as a function of time at ~163 and ~308 °C for the catalyzed and noncatalyzed MgH_2, respectively, which were deduced by the TG measurements. It can be seen that the HD curve of Ni^{nano}-catalyzed MgH_2 is of exponential type, while that of noncatalyzed MgH_2 is of sigmoid shape, the same as for nonmilled MgH_2 itself.[25] In this work, it takes more than 200 min at 308 °C to reach complete hydrogen desorption from noncatalyzed MgH_2 after milling for 15 min. Results in the literature indicate that the desorption times of milled MgH_2 are typically between 30 and 100 min at 300 °C.[11,24] However, it should be noted that all of those data were examined after milling for longer time than 15 min. Therefore, it seems that longer milling leads to better kinetics for noncatalyzed MgH_2 by creating activated surface. On the other hand, after catalyzing by 2 mol % Ni^{nano} on MgH_2, it is noteworthy that 90% of hydrogen is desorbed within 100 min at 163 °C under He gas flow with no partial pressure of hydrogen, indicating drastic improvement of the kinetics. It should be described in this connection that 90% of hydrogen is absorbed within 15 min at the same temperature under a hydrogen gas pressure of 3 MPa vice versa.

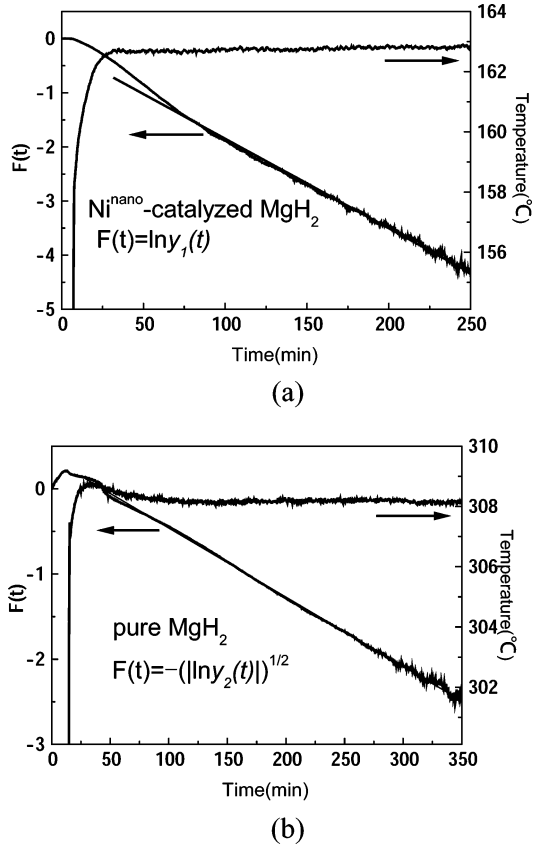

Figure 9. Normalized residual hydrogen function *F(t)*, and the aspect of temperature fluctuation around fixed temperatures as a function of HD reaction time for (a) the 2 mol % Ni^{nano}-catalyzed MgH_2 composite prepared by milling for 15 min at 200 rpm and (b) the pure MgH_2 milled for 15 min at 200 rpm, respectively.

On the basis of the above results, modified residual hydrogen functions, $F_1(t) = \ln y_1(t)$ and $F_2(t) = -(|\ln y_2(t)|)^{1/2}$ are plotted as a function of time in Figure 9, where $y_1(t)$ and $y_2(t)$ indicate residual hydrogen concentrations ($0 \le y \le 1$) normalized by the hydrogen content at $t = 0$ for the catalyzed and noncatalyzed MgH_2, respectively. It can be seen that both the functions linearly decrease with increasing time, after the sample temperatures have reached the programmed ones of about 163 and 308 °C, respectively. For the Ni^{nano}-catalyzed MgH_2, the good linearity in Figure 9a indicates that the desorbing reaction is a first-order one. Huot et al.[5] have so far claimed that the hydrogen desorption reaction for 5 mol % TM^{micro}-doped MgH_2 where TM = Ti, V, Mn, Fe, and Ni at 250 °C under 0.015 MPa followed the interface controlling law of $[1 - y^{1/2}] = kt$. Appearance of the first-order reaction in this work might be ascribed to the catalytic effect of the nanoparticle Ni metal on the sample surface. Generally, it is well-known that the first-order reaction obeys the following differential equation

$$\frac{dy}{dt} = -ky \tag{1}$$

where k is the reaction rate constant; that is, the HD reaction rate is proportional to the residual hydrogen content. On the other hand, for the noncatalyzed MgH_2, $F_2(t) = -(|\ln y_2(t)|)^{1/2}$ linearly changes as a function of time as shown in Figure 9b. This function has been generally expressed as the Johnson−Mehl−Avrami (JMA) equation for a nucleation and growth process[21−23] and the exponent $^1/_2$ might mean either zero nucleation rate and two-dimensional growth of nuclei or a constant nucleation rate and one-dimensional growth of nuclei as a rate-determining step. In some papers, it has been concluded that the rate-determining step of the HD reaction for pure MgH_2 was the nucleation and growth of Mg phase on the basis of similar experimental results to ours.[24−25] In other words, these considerations by means of the JMA equation are based on the dynamics of inner MgH_2 particle like nucleation and growth. However, we have only modified the surface condition of the MgH_2 powder by Ni catalyst and HD reaction was significantly improved and transformed into a first-order one. Since Mg has no strong catalytic effect for dissociating H_2 molecule into H atoms on the surface vice versa,[26] the recombination process on the MgH_2 surface should be taken into account as a rate-determining step of the HD reaction for pure MgH_2.

Hence, to systematically understand the HD reaction kinetics for noncatalyzed MgH_2 as well as catalyzed MgH_2, a new HD reaction model is necessary and proposed in this paper. Then, we assume that the HD reaction from MgH_2 to Mg + H_2 follows a modified first-order reaction model, in which a surface condition is taken into account. As the surface condition, we introduce an activated surface area $1 - \theta(t)$ and a nonactivated surface area $\theta(t)$on the noncatalyzed MgH_2 powder, which are normalized by a total surface area. On the activated surface area, we assume that hydrogen atoms are easily recombined into hydrogen molecules and are released into He flow gas. Furthermore, we assume that the nonactivated surface area $\theta(t)$ is an exponential type decreasing function for reaction time as follows

$$\theta(t) = \exp(-\nu t) \tag{2}$$

where ν is a reaction rate constant. Thus, the activated surface area $1 - \theta(t)$ increases with time evolution and finally reaches to 1. This assumption suggests that the recombination rate of H_2 on the surface gradually increases with the increasing time by a surface modification during the HD reaction. Microscopic behavior of the surface modification during HD reaction is considered that the MgO layers on the MgH_2 surface are reduced by desorption hydrogen to Mg or the surface structure of nonactivated surface is reconstructed to activated surface.

Therefore, the HD rate of noncatalyzed MgH_2 should be proportional to both the normalized residual hydrogen content *y(t)* and the activated surface factor $1 - \theta(t)$, as follows

$$\frac{dy}{dt} = -ky(1 - \theta(t)) \tag{3}$$

By integrating eq 3, we can obtain the following expression

$$\ln y = -k\int_0^t [1 - \exp[-\nu t]]dt \tag{4}$$

Actually, in the case of pure milled MgH_2, we can well fit the desorption reaction by eq 4. Here, if $\nu t \ll 1$, then $1 - \theta(t)$is expanded as $1 - \exp(-\nu t) = \nu t - (\nu t)^2/2 + (\nu t)^3/6 \ldots \cong \nu t$. Then, eq 4 is rewritten as follows:

$$\ln y \cong -k\int_0^t \nu t\, dt = -\frac{1}{2}k\nu t^2 \tag{5}$$

By transforming eq 5, we obtain the following equation, that is the same function as $F_2(t)$

$$F_2(t) = -(|\ln y|)^{1/2} = at, \text{ where } a = -\sqrt{\frac{1}{2}k\nu} \tag{6}$$

Thus, we can understand the HD reaction of MgH_2 by the modified first-order model, in which the surface activation condition is taken into account as well. From the experimental

data, we deduced the value of $\nu t_{max} \cong 0.008$, $t_{max} = 260$ min, which really satisfies the condition of $\nu t \ll 1$ in the above assumption.

In the case of the Ni^{nano}-catalyzed MgH_2, we can also understand the HD reaction using the modified first-order model. Then, it is considered that the nonactivated surface area is $\theta(t) = 0$ at any time, because the 3d-transition metal Ni^{nano} has a strong catalytic effect for recombining H atoms to H_2 molecules. Therefore, the activated surface area is $1 - \theta(t) = 1$ at any time in eq 2, and the desorption reaction rate should be described by eq 1, being a first-order reaction.

3.5. Estimation of Activation Energy in Pure MgH_2 and Ni^{nano}-Catalyzed MgH_2 Composite. If the HD reaction as a function of time is described by eqs 1 and 3, we can estimate the activation energy, E, by the Kissinger method[27] according to the following consideration. In the constant heating process, such as $T = T_0 + \beta t$, where T_0 is the initial temperature of the reaction and β the heating rate, eq 3 (where $1 - \theta(t) \approx \nu t$) for the modified first-order reaction is generalized to

$$\frac{dy}{dT} = -\frac{1}{\beta} k y \nu \frac{T}{\beta} \tag{7}$$

Here, k and ν can be respectively expressed by the Arrhenius equation as follows:

$$k(T) = k_0 \exp[-(E_{A1}/RT)] \tag{8}$$

$$\nu(T) = \nu_0 \exp[-(E_{A2}/RT)] \tag{9}$$

Here k_0 and ν_0 are the frequency factors, R the gas constant, E_{A1} and E_{A2} the activation energies for the HD process with an activated surface and the surface activating process, respectively. By substituting eqs 8 and 9 into eq 7, we obtain the following equation:

$$\frac{dy}{dT} = -k_0 \nu_0 \exp\left[-\frac{E_{A1} + E_{A2}}{RT}\right] y \frac{T}{\beta^2} \tag{10}$$

Using the substitutions of $K_0 = k_0 \nu_0$, $E_A = E_{A1} + E_{A2}$, we obtain

$$\frac{dy}{dT} = -K_0 \exp\left[-\frac{E_A}{RT}\right] y \frac{T}{\beta^2} \tag{11}$$

The maximum desorption fraction rate is found by making $d^2y/dT^2 = 0$, and thus we obtain the relationship

$$\exp\left[-\frac{E_A}{RT}\right] = \frac{\beta^2}{K_0 T^2}\left[\frac{E_A}{RT} + 1\right] \tag{12}$$

If we assume that $E_A/RT \geq 1$ (usually $E_A/RT \cong 100$), it is possible to put $E_A/RT + 1 \cong E_A/RT$, and then we obtain the following equation:

$$\ln[\beta^2/T_P^3] = -E_A/RT_P + \ln[K_0 R/E_A] \tag{13}$$

From eq 1 for the first order reaction, we similarly obtain the usual Kissinger equation as follows:

$$\ln[\beta/T_P^2] = -E_{A1}/RT_P + \ln[k_0 R/E_{A1}] \tag{14}$$

Using the different Kissinger equations, (13) or (14), the activation energy E_A and E_{A1} was estimated for the pure and catalyzed MgH_2, respectively, as follows. We measured the TDMS profiles at several heating rates from 1 to 20 °C/min as a function of temperature for noncatalyzed and Ni^{nano}-catalyzed MgH_2. The results are plotted in Figure 10, parts a and b. From the peak temperature T_P observed at the heating rate of β, the Kissinger plots, i.e., ln $[\beta^2/T_P^3]$ and ln $[\beta/T_P^2]$ as a function of the inverse of T_P are given in Figure 11, parts a and b for noncatalyzed and catalyzed MgH_2, respectively. From the slope of these straight lines, the activation energies of E_A and E_{A1} were estimated to be 323 ± 40 kJ/molH_2 and 94 ± 3 kJ/molH_2, respectively. The difference value of ~230 kJ/molH_2 between these activation energies indicates the activation energy of E_{A2} corresponding to surface activation process in pure MgH_2. Thus, Ni^{nano}-catalyzed MgH_2 possessing the activated surface significantly decreases the activation energy of hydrogen desorption.

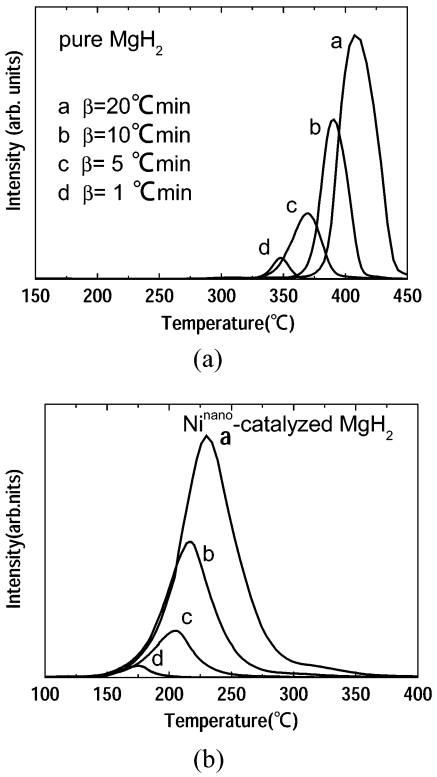

Figure 10. Thermal desorption mass spectra of hydrogen under various heating rates (β = 1,5,10,20 °C/nim) from (a) the pure MgH_2 milled for 15 min at 200 rpm and (b) the 2 mol % Ni^{nano}- catalyzed MgH_2 composite prepared by milling for 15 min at 200 rpm, respectively. The intensities of the longitudinal axes indicate the amount of hydrogen desorption per unit time.

Fernández et al.[25] also have determined the activation energy in the HD process for the pure MgH_2 by deducing the reaction rate constant k at several different temperatures assuming the Johnson−Mehl−Avrami (JMA) equation for a nucleation and growth process model. The estimated value was ~160 kJ/molH_2, which is much smaller than our estimated one. This disagreement may be due to the difference between the used models. Because if we adapt the first-order reaction model without considering surface activation process, the activation energy is deduced to be 159 ± 20 kJ/molH_2 using the usual Kissinger plot from our experimental data, which is corresponding to almost the same value with Fernández's estimation.

Conclusion

In this work, the hydrogen desorption (HD) properties of the catalyzed MgH_2 composite prepared by mechanically milling the mixture of MgH_2 and a small amount of Fe^{nano}, Co^{nano}, Ni^{nano}, and Cu^{nano} nanoparticle metals as a catalyst were carefully

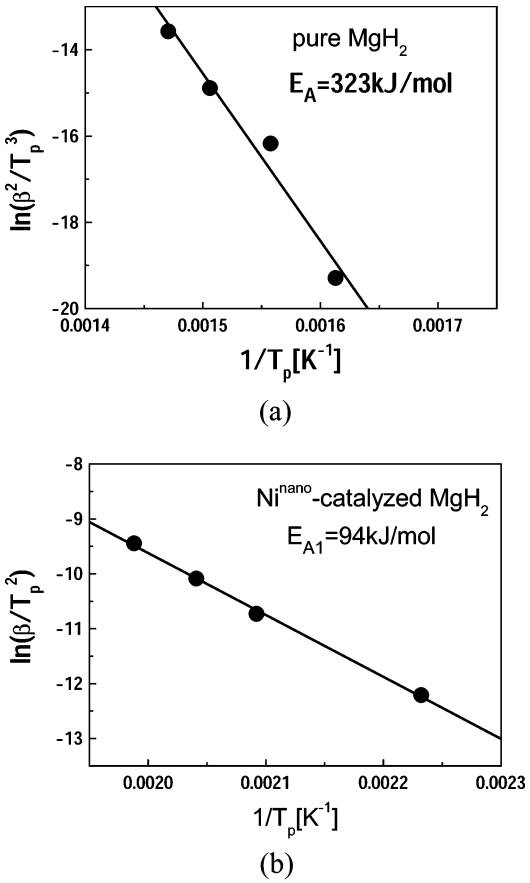

Figure 11. Two kinds of Kissinger plots for the hydrogen desorption reaction for (a) pure MgH_2 milled for 15 min at 200 rpm and (b) the 2 mol % Ni^{nano}-catalyzed MgH_2 composite prepared by milling for 15 min at 200 rpm, respectively. Notations: T_p indicates the peak temperatures in thermal desorption spectra (a and b), respectively.

examined. All the catalyzed MgH_2 composite showed much better HD properties than the pure milled MgH_2 by only 2 h of milling. In paricular, the 2 mol % Ni^{nano}-doped MgH_2 composite prepared by soft milling for a short milling time of 15 min under a slow milling revolution speed of 200 rpm shows the most superior hydrogen storage properties: The product has a quite sharp peak at ~200 °C in the TDMS curve and a large amount of hydrogen (~6.5 wt %) is desorbed in the temperature range from 150 to 250 °C under a heating rate of 5 °C/min. The EDX micrographs corresponding to Mg and Ni element profiles indicated that a small amount of nanoparticle Ni^{nano} metals homogeneously dispersed on the surface of MgH_2.

We confirmed that the Ni^{nano}-catalyzed product revealed better reversible hydriding and dehydriding cycles at 150 °C than those at 200 °C, though the second cycle data is slightly worse than that after first cycle after milling. This degradation at 200 °C is due to the fact that Mg_2Ni phase grows up in the boundary between MgH_2 phase and Ni catalyst after hydrogen was desorbed at 200 °C. From the studies of kinetics, the HD reactions in noncatalyzed and Ni^{nano}-catalyzed MgH_2 could be understood by the modified first-order model, in which the surface activation condition was taken into account.

In addition, from the Kissinger plots, the activation energy was estimated to be 323 ± 40 and 94 ± 3 kJ/molH_2 for the noncatalyzed and the catalyzed MgH_2, respectively. The activation energy of surface activation process on the MgH_2 surface in the HD reaction was estimated to be ~230 kJ/mol, which is the difference value between these activation energies. This indicates that the catalytic effect due to Ni^{nano}-doping significantly decreases the activation energy for hydrogen desorption by surface activation.

Acknowledgment. This work was supported by the project "Development for Safe Utilization and Infrastructure of Hydrogen Industrial Technology" in the New Energy and Industrial Technology Development Organization (NEDO), Japan, and by a Grant-in-Aid for COE Research (No. 13CE2002) from the Ministry of Education, Sciences, and Culture of Japan.

References and Notes

(1) Cummings, D. L.; Powers, G. J. *Ind. Eng. Chem., Process Des. Dev.* **1974**, *13*, 182.
(2) Stampfer, J. F., Jr.; Holley, C. E., Jr.; Suttle, J. F. *J. Am. Chem. Soc.* **1960**, *82*, 3504.
(3) Vigeholm, B.; Kjoller, J.; Larsen, B.; *J. Less-Common Met.* **1980**, *74*, 341.
(4) Liang, G.; Huot, J.; Boily, S.; Van Neste, A.; Schulz, R. *J. Alloys Compd.* **1999**, *291*, 295.
(5) Liang, G.; Huot, J.; Boily, S.; Van Neste, A.; Schulz, R. *J. Alloys Compd.* **1999**, *292*, 247.
(6) Liang, G.; Huot, J.; Boily, S.; Schulz, R. *J. Alloys Compd.* **2000**, *305*, 239.
(7) Dehouche, Z.; Djaozandry, R.; Huot, J.; Boily, S.; Goyette, J.; Bose, T. K.; Schulz, R. *J. Alloys Compd.* **2000**, *305*, 264.
(8) Huot, J.; Pelletier, J. F.; Liang, G.; Sutton, M.; Schulz, R. *J. Alloys Compd.* **2002**, *330*−*332*, 727.
(9) Zaluska, A.; Zaluski, L.; Ström-Olsen, J. O. *J. Alloys Compd.* **1999**, *288*, 217.
(10) Kanoya, I.; Hosoe, M.; Suzuki, T. *Honda R & D Tech. Rev.* **2002**, *14*, 91.
(11) Oelerich, W.; Klassen, T.; Bormann, R. *J. Alloys Compd.* **2001**, *315*, 237.
(12) Oelerich, W.; Klassen, T.; Bormann, R. *Adv. Eng. Mater.* **2001**, *3*, 487.
(13) Dehouche, Z.; Klassen, T.; Oelerich, W.; Goyette, J.; Bose, T. K.; Schulz, R. *J. Alloys Compd.* **2002**, *347*, 319.
(14) Barkhordarian, Gagik; Klassen, Thomas; Bormann, Rüdiger. *Scr. Mater.* **2003**, *49*, 213.
(15) Higuchi, K.; Yamamoto, K.; Kajioka, H.; Toiyama, K.; Honda, M.; Orimo, S.; Fujii, H. *J. Alloys Compd.* **2002**, *330*−*332*, 526.
(16) Fujii, H.; Higuchi, K.; Yamamoto, K.; Kajioka, H.; Orimo, S.; Toiyama, K. *Mater. Trans.* **2002**, *43*, 2721.
(17) Gutfleisch, O.; Schlorke-de Boer, N.; Ismail, N.; Herrich, M.; Walton, A.; Speight, J.; Harris, I. R.; Pratt, A. S.; Züttel, A. *J. Alloys Compd.* **2003**, *356*−*357*, 598.
(18) Bobet, J−L.; Chevalier, B.; Song, M. Y.; Darriet, B.; Etourneau, J. *J. Alloys Compd.* **2003**, *336*, 292.
(19) Hanada, Nobuko; Ichikawa, Takayuki; Orimo, Shin-Ichi; Fujii, Hironobu. *J. Alloys Compd.* **2004**, *366*, 269.
(20) Harris, J.; Andersson, S. *Phys. Rev. Lett.* **1985**, *55*, 1583.
(21) Avrami, M. *J. Chem. Phys.* **1939**, *7*, 1103.
(22) Avrami, M. *J. Chem. Phys.* **1940**, *8*, 212.
(23) Avrami, M. *J. Chem. Phys.* **1941**, *9*, 177.
(24) Huot, J.; Liang, G.; Boily, S.; Van Neste, A.; Schulz, R. *J. Alloys Compd.* **1999**, *293*−*295*, 495.
(25) Fernández, J. F.; Sánchez, C. R. *J. Alloys Compd.* **2002**, *340*, 189.
(26) Schlapbach, L., Ed. *Hydrogen in Intermetallic Compounds 2*; Springer-Verlag: Berlin, 1992; p 69.
(27) Kissinger, H. E. *Anal. Chem.* **1957**, *29*, 1702.